Journal of the European Ceramic Society 18 (1998) 1905–1914

PII: S0955-2219(98)00129-0
0955-2219/98/$—see front matter

Near Net Shape Manufacturing of Polymer Derived Ceramics

Peter Greil*

University of Erlangen-Nuernberg, Department of Materials Science (Glass and Ceramics), Martensstr. 5, D-91058 Erlangen, Germany

Abstract

Pyrolytic conversion of preceramic polymers loaded with active filler particles offers the possibility of near net shape manufacturing of bulk ceramic components from polymers. Active fillers based on elements (B, Si, Al, Ti, Mo, etc.), intermetallics ($CrSi_2$, $MoSi_2$, etc.) or ceramic compounds (AlN, B_4C, etc.) which react with the solid and gaseous decomposition products of the preceramic polymer (polysilane, -carbosilane, -silazane, siloxane, etc.) during pyrolysis may form carbide, nitride or oxide reaction products in the polymer derived amorphous or microcrystalline matrix. The main effects of the active fillers are to form a stabilizing network of the filler reaction products, increase ceramic yield of the polymer, and to provide internal surface for material transport during polymer decomposition reactions. Thus, dimensional change, porosity formation as well as material properties can be tailored in a wide range by combination of a variety of polymers, fillers and reaction atmospheres. © *1998 Elsevier Science Limited. All rights reserved*

1 Introduction

Formation of novel ceramic materials from Si-containing polymers [$R_{1\ldots2}$,$Si(C,N,B,O)_{0.5\ldots1.5}$] where R is an organic functional group (for example alkyl, aryl, etc. group) has attained particular interest because of high purity precursor materials, applicability of versatile plastic shaping technologies and low manufacturing temperatures.[1–15] Suitable precursor polymers of high ceramic yield are based on cross-linked poly(silanes), -(carbosilanes), -(silazanes), -(siloxanes) and molecular mixtures thereof Preceramic polymers of high ceramic yield (more than 50 wt% of the inital polymer weight are retained in the ceramics residue) have been developed as novel binders for ceramic powders,[16] for joining of SiC to SiC,[17] for synthesis of ultrafine powders,[18] for matrix formation in fiber reinforced ceramic composites [19–21] and for production of coatings[10] and ceramic fibers.[2,12,22,23]

Bulk ceramic compents, however, could not be manufactured yet due to an inherent density increase from 1 to 3 g cm^{-3} (depending on the ceramic phase) during pyrolytic polymer–ceramic conversion. While for unconstrained relaxation of the structural rearrangement processes from viscous polymer to rigid ceramic a tremendous shrinkage of up to 80 vol% can occur, pores and cracks are likely to form when this shrinkage ist constrained by the increasing stiffness of the ceramic residue. Loading the polymer matrix with active filler (F) particles, which undergo a volume expansion upon reaction with the decomposition fragments of the polymer (solid carbon and gaseous carbon hydroxides like CH_4 C_2H_4 C_6H_6, etc. depending on the polymer composition) or a reactive gas atmosphere (for example N_2, NH_3, CH_4, O_2, etc.), near net shape manufacturing of components with complex geometry becomes possible. Figure 1 shows the basic concept of the active filler controlled polymer pyrolysis process (AFCOP).[24–29]

The filler particles form a stabilizing rigid network in the low viscous polymer phase, offer a large interface area for material transport during polymer decomposition and increase the ceramic yield of the polymer due to reaction with the gaseous decomposition products. Suitable active fillers are elements or compounds forming carbide, nitride, or oxide reaction products such as Al, B, Si, Ti, $CrSi_2$ $MoSi_2$, etc. which exhibit a high specific volume increase upon reaction,[25] Table 1. Ceramic fillers like AlN, B_4C, etc. offer the possibility of forming matrices of the sialon, mullite or borosilicate type when reacting with the siloxane polymer, for example. When metal oxide fillers such as NiO, Mn_2O_3, CuO, etc. are used, reduction of the active filler results in the formation of novel ceramic composite materials containing highly dispersed metal or metal silicide particles. The active fillers can be combined or partly replaced by inactive

*To whom correspondence should be addressed.

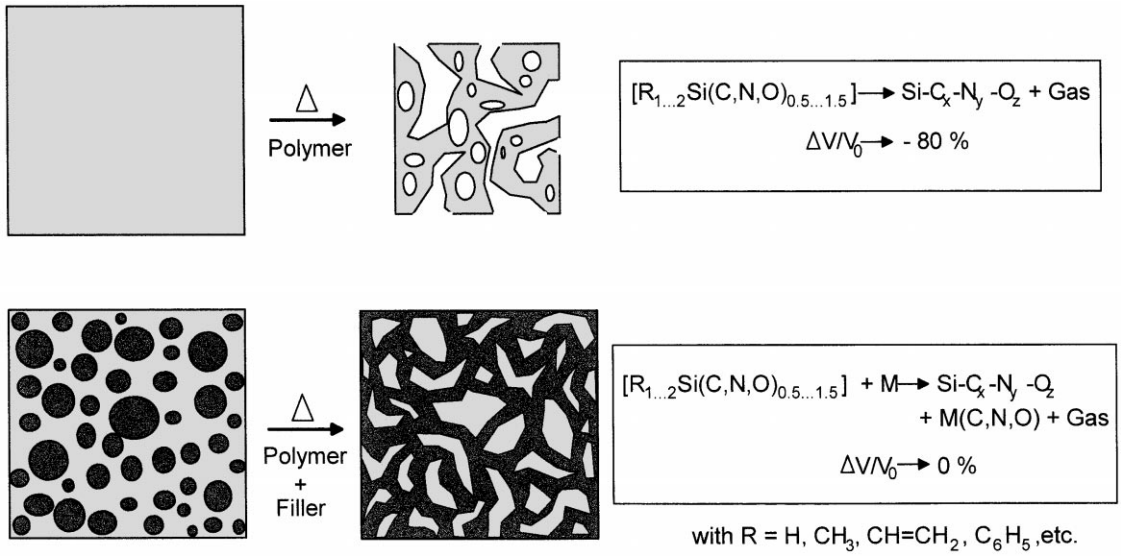

Fig. 1. Basic principle of net shape polymer–ceramic conversion by active filler controlled pyrolysis.

Table 1. Molar volume changes of potential active filler systems. Reactants are solid carbon, gaseous hydrocarbons or reactive gas atmospheres (nitrogen, oxygen)

Specific volume changes of active fillers (1%)				
Reactant	C(s)	C(g)	N_2(g)	O_2(g)
Ti	−24	+14	+8	+78
Zr	−21	+9	+3	+40
Mo	−5	+22	—	
Al	+9	+53	+26	+28
B	−7	+20	+142	—
Si	−30	+7	+13	+88
$MoSi_2$	−4	+48	—	—
$CrSi_2$	−7	+54	+23	+69
$TiSi_2$	−10	+47	+53	+171

fillers which do not react during the pyrolysis process but can provide specific functionality to the ceramic material. Thus, for adjusting elasticity, thermal expansion, electrical resistance, etc. inactive fillers offer an additional degree of freedom for tailoring the material properties. While for the active fillers typical grain sizes are in the range of 1 to 10 μm, inert fillers with a particle size down to the nm-range can be processed. Based on the active filler controlled polymer pyrolysis process a variety of ceramic microcomposite materials such as SiOC/TiC, SiOC/TiN, SiOC/SiC, SiOCN/BN, SiOC/(Cr_3,C_2,Si_3N_4,), or SiOC/Mo_2C and SiOC/TaC, have yet been manufactured as bulk components, as the matrix in fiber reinforced composites, or as surface coatings of porous substrate materials.[26,29–32] While all of the above mentioned materials were fabricated from polysiloxane polymers, oxygen poor nano-composite materials such as SiC/Si_3N_4 and SiC/B_4C could be formed by using Si and B filled polysilane as the precursor system.[33] Polysilazane, polycarbosilane and borane-containing polymers have also been used as reactants with active fillers.[34]

The results presented in the following discussion are focused on the specific microstructure formation processes e.g. polymer/filler reactions, shrinkage/porosity relations and microstructure/property dependencies. Only poly(siloxanes) containing various active filler phases will be considered, although, the concept of filler/polymer reaction can be applied to oxygen free poly(carbosilanes), and -(silazanes) as well.

2 Experimental procedure

Manufacturing of bulk components involves the formation of homogeneous polymer/filler powder mixtures or slurries, shaping, curing, green machining, and finally pyrolysis. Commercial poly(siloxanes) containing either methyl (NH 2100, Chemiewerke Nuenchritz, GE) or phenyl (H 62 C, Wacker Chemie, Burghausen, GE) groups were loaded with 20–60 vol% of various active fillers (see Table 1) with mean particle sizes in the range 1–3 μm. Both poly(siloxane) polymers exhibit curing temperatures near 200°C. Curing of NH 2100 proceeds via a condensation reaction of Si–OH groups resulting in the release of H_2O. Thus, curing has to be carried out under pressure to avoid uncontrolled bubble formation. H 62 C contains vinyl groups which allow pressure-free curing via a hydrosilylation reaction.[24] Although the oxygen containing composite ceramics derived from poly(-siloxanes) are restricted to application temperatures <1200°C, they offer significant advantages over oxygen poor high temeprature polymers like poly(carbosilanes), (-silazanes) or -(borosilazanes).

Poly(siloxanes) are available on an industrial scale at a low price level, can be processed easily under ambient conditions and provide a high ceramic yield of 70 wt% or more.

Liquid or solid polymer precursors are mixed with active filler powders to obtain homogeneous suspensions with a rheological behavior suitable for various shaping technologies. Transition metals and intermetallic compounds, however, can act as catalysts in various polymerization processes.[36] Thus, filler surface chemistry has a strong impact on curing temperatures and viscosity/temperature dependencies. Using injection moulding, for example, granulates of the polymer/filler mixture have to be prepared by extrusion. Surface coating of the filler particle by carboxylic acids such as citric or tartraric acid has been succesfully applied to avoid uncontrolled curing of the polymer phase and to achieve appropriate viscosities for injection moulding.[28] Figure 2 summarizes the processing scheme for polymer/filler mixtures used as starting materials for near net shape manufacturing of polymer derived ceramics.

A variety of conventional as well as novel shaping techniques can be applied to the polymer/filler-systems. Pressing of granulated powders, where the filler powder is coated with the solid polymer phase, can be used to produce simple shaped products. Components of complex shape may be formed by injection moulding and casting. Porous preforms can be impregnated using low viscous slurries. For fiber reinforced composite manufacturing low viscous polymer/filler slurries were prepared in order to coat the fiber filaments prior to winding or to infiltrate a porous fiber preform according to the resin transfer moulding (RTM) process. Polymer/filler systems may further be of particular interest for novel solid free-form fabrication technologies such as selective laser sintering, multilayer jet printing, laminated object manufacturing or stereolithography. Selective laser sintering of active filler loaded polycarbosilanes has been demonstrated to form crack free layers of silicon carbide based composites.[35]

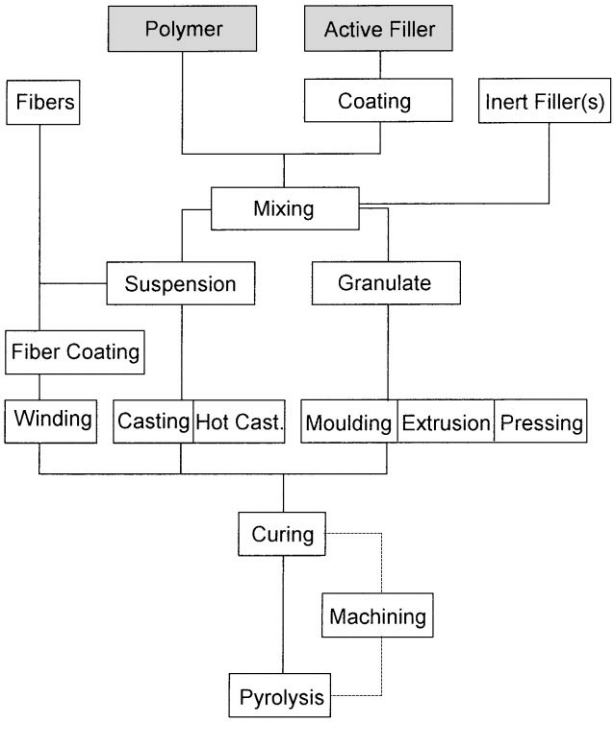

Fig. 2. Processing scheme of polymer/filler-derived ceramics.

After shaping the cured (green) compact can be machined by conventional surface machining techniques (CNC). Polymer to ceramic conversion is achieved by heating in a flowing inert (Ar, He) or reactive (N_2 NH_3, CH_4) atmosphere at temperatures typically between 1000 and 1500°C. The heating cycle may involve one or more annealing steps at lower temperatures which are of particular importance for release of polymer decomposition products via an open pore network and for the nucleation of the filler reaction product phases. A typical pyrolysis cycle involves heating with 5°C min^{-1}, holding at 600°C for 1 h, heating up to the peak temperature of 1400°C with the same heating rate, a dwell time of 1–3 h and subsequent cooling with 5°C min^{-1}.

3 Results and Discussion

3.1 Polymer/filler-reactions

During heating the weight loss associated with pyrolytic decomposition of the cured preceramic polymer starts at 400°C in argon as well as in nitrogen atmosphere. From mass spectroscopy of cross-linked polysiloxane resins, release of hydrocarbons like benzene C_6H_6, methane CH_4, etc has been detected between 400 and 800°C, and hydrogen from 600 to 1100°C, resulting from cleavage of Si–H, Si–C, and CH bonds. Total weight loss of the polymer phase attains 20–30 wt% up to 1400°C. Pyrolysis of the poly(siloxane) preceramic polymer phase generally involves several distinct steps: (i) an organic–inorganic transformation between 600 and 800°C, leading to an amorphous hydrogenated oxycarbide built on tetrahedral structures of the type $Si(C_aO_b)$ with $a + b = 4$, depending on the initial polymer composition;[12,13] (ii) precipitation of excessive carbon to form a network of turbostratic carbon[37] above 800°C; (iii) nucleation of crystalline precipitations such as SiC and SiO_2, between 1100 and 1600°C and (iv) grain coarsening that results in consumption of the residual amorphous phase and reduction of oxygen content due to evaporation of SiO and CO.[38] Devitrification of the amorphous SiOC-phase

$$\mathrm{Si-O}_a-\mathrm{C}_b(\mathrm{am})(\mathrm{s}) \rightarrow \left(1-\frac{1}{2}\right)\mathrm{SiC(s)} + \frac{a}{2}\mathrm{SiO_2(s)} + \left(\frac{a}{2}+b-1\right)\mathrm{C(s)} \quad (1)$$

will induce irreversible property changes of the polymer derived matrix phase such as elasticity, creep resistance and fracture behavior.

In the case of poly(siloxane) NH2100, for example, analyses of elemental distribution by electron paramagnetic resonance spectroscopy (EPR) and chemical analyses indicate, that from room temperature to 1400°C loss of hydrocarbon species results in a shift of hypothetical monomer $[\mathrm{Si}(\mathrm{C}_a\mathrm{O})_b]$ composition from the $[\mathrm{SiC_2O_2}]$–$[\mathrm{CC_4}]$ line to $[\mathrm{SiCO_3}]-[\mathrm{CC_4}]$ line. Simultaneously, the mean number of Si–C-bonds per Si atom (a in monomer stochiometry) decreases from approximately 2 at 600°C to less than 1·5 at 1000°C with a further decrease at higher temperatures.

Depending on their reactivity, the filler particles begin to react with solid or gaseous decomposition products at 400°C (Ti) or 1300°C (B). In the presence of a reactive filler, solid carbon and gaseous hydrocarbon species can react to form carbide phases resulting in a significant increase of ceramic yield

$$[\mathrm{RSiO_{1.5}}](\mathrm{s}) + \mathrm{F(s)} \rightarrow \mathrm{Si-O-C(s)} + \mathrm{FC}_x\mathrm{(s)} + \mathrm{H_2(g)} \quad (2)$$

For example, poly(phenylsiloxane) loaded with Ti and pyrolzed in Ar-atmosphere at 1000°C yields a siliconoxycarbide composite [26]

$$\left[\left(\mathrm{C_6H_5}\right)\mathrm{SiO_{1.5}}\right](\mathrm{s}) + \mathrm{Ti(s)} \rightarrow \mathrm{Si-O-C(s)} + \mathrm{TiC(s)} + \mathrm{CH}_x\mathrm{(g)} + \mathrm{H_2(g)} \quad (3)$$

where CH_x mainly represents $\mathrm{C_6H_6}$. Due to the reaction of Ti with the gaseous hydrocarbon species the ceramic yield of the polymer phase was found to be 10% higher compared to the filler free polymer pyrolysis. When pyrolysis is carried out in a reaction atmosphere, the filler particles can react with the gaseous phase present in the open pore network, which forms during polymer decomposition between 400 and 800°C (transient porosity) or due to carbothermal decomposition at temperatures above 1000°C. For example, reaction of poly(phenylsiloxane) with $\mathrm{CrSi_2}$ in $\mathrm{N_2}$-atmosphere at 1400°C yields an oxycarbonitride ceramic composite

$$[(\mathrm{C_6H_5})\mathrm{SiO_{1.5}}](\mathrm{s}) + \mathrm{CrSi_2(s)} + \mathrm{N_2(g)} \rightarrow \mathrm{Si-O-C-N(g)} + \mathrm{Cr_3C_2(s)} + \mathrm{Si_3N_4(s)} + \mathrm{CH}_x\mathrm{(g)} \quad (4)$$

If the carbon activity at the filler particle surface is sufficiently high ($a_c > 0{\cdot}1$), carbon generated by polymer decomposition reacts with chromium, whereas silicon reacts with nitrogen from the reactive atmosphere to form a carbide/nitride scale of the $\mathrm{Cr_3C_2}$-$\mathrm{Si_3N_4}$ type on the filler particle surface. The driving force to form nitrides can be increased with increasing external nitrogen pressure.[24] Reaction of poly(methylsiloxane) with B in $\mathrm{N_2}$-atmosphere at 1500°C

$$\left[\left(\mathrm{CH_3}\right)\mathrm{SiO_{1.5}}\right](\mathrm{s}) + \mathrm{B(s)} + \mathrm{N_2(g)} \rightarrow \mathrm{Si-O-C-N(s)} + \mathrm{BN(s)} + \mathrm{Si_2N_2O(s)} + \mathrm{CH}_x\mathrm{(g)} \quad (5)$$

results in the formation of nitride and oxynitride reaction products. Due to a specific volume increase of +39% from $\mathrm{CrSi_2}$ to $(\mathrm{Cr_3C_2}+\mathrm{Si_3N_4})$ and even +142% from B to BN zero shrinkage polymer-ceramic transformation can be obtained with volume fractions of 30–40%, Fig. 3. Due to lower molar volume changes other fillers such as $\mathrm{MoSi_2}$, Si, $\mathrm{TiSi_2}$, Ti, Table 1, need significantly higher initial volume fractions to achieve zero shrinkage.

Shrinkage is strongly affected by kinetic effects of filler particle reaction e.g. temperature and time. Reaction of the filler particle can be described according to the shrinking core model,[39] where the time to fully react the filler particle with the initial particle radius R^f and density ρ^F with a gas phase of concentration C_{gas} can be expressed by the specific

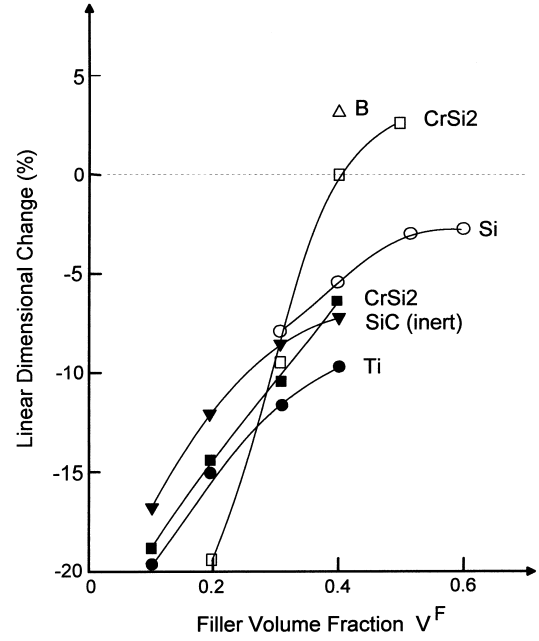

Fig. 3. Linear dimensional change of poly(siloxane) loaded with different active fillers after pyrolysis at 1400–1500°C in nitrogen (○) or argon (●) atmosphere.

mass transfer coefficient (gas–solid), k_g, the first order rate constant for surface reaction, k_s, and the effective diffusion coefficient of gaseous reactant, D,

$$t = \frac{\rho^F R^F}{bC_{\text{gas}}}\left(\frac{1}{3K_g} + \frac{1}{K_s}\frac{R}{6D}\right). \quad (6)$$

Although it is not possible to assign values to these constants for the particular systems considered in this work, general trends for affecting the filler reaction can be derived from eqn (6). With decreasing particle size, filler reaction time is reduced so that, within a given reaction time, a higher fraction of smaller particles is transformed compared to larger particles, and hence, reduction of overall shrinkage is higher. Increasing the temperature, the rate constants k_g, k_s and D increase by $\exp(-Q/kT)$ so that thermally activated processes will be accelerated accordingly. Similarly, prolonged annealing time also results in reduced shrinkage as shown in Fig. 4 for a B-filled polysiloxane.

3.2 Shrinkage and porosity

Generally, zero shrinkage could only be obtained in the presence of a certain amount of residual prosity. Figure 5 summarizes experimental data of linear shrinkage and porosity observed in a variety of examined polymer/filler-systems. Assuming complete polymer and filler reaction, critical volume fractions of filler necessary to achieve zero shrinkage can be calculated according to an isotropic volume balance model.[25] Taking into account the specific molar volume changes of the polymer matrix, Ψ^P, and the filler phase, Ψ^F, upon decomposition and reaction as well as formation of residual porosity, P, the total volume change of the composite, Ψ^*, is given by

$$\Psi^* = \left(1 - \frac{V^F}{V_C^F}\right)(\Psi^P - 1) + V^F(\Psi^F - 1) + P \quad (7)$$

Thus, for zero shrinkage ($\Psi^* = 0$) a filler volume fraction V^F results

$$V^F = \frac{(\Psi^P - 1) - P}{\left(\frac{\Psi^P - 1}{V_C^F}\right) - (\Psi^F - 1)} \quad (8)$$

V_C^F represents a maximum packing density of the filler powder in the polymer/ filler-mixture ($V^F{}_c \rightarrow 0{\cdot}5$). For some of the preceramic polymers values for Ψ^P can be found in the literature,[24] showing that typical values are in the range of $\Psi^P \approx 0{\cdot}25 - 0{\cdot}5$. The general trends in material behavior predicted from eqn (8) are drawn in Fig. 6 and compared to the specific volume change of various filler systems upon reaction pyrolysis.

Porosity formation is strongly affected by the presence of filler particles. While in low dimensional ceramic SiC-fibers fabricated from filler free preceramic poly(carbosilanes), closed pores of less than 5 nm were detected using small angle X-ray scattering,[40] significantly larger pores and cracks with diameters up to the mm range occur in filler free bulk materials. In the presence of fillers, however, porosity formation is strongly affected by the filler surface and the filler reaction upon pyrolysis. Figure 7 shows the development of transient porosity during pyrolysis of poly(vinylmethylphenyisiloxane) loaded with different volume fractions of $CrSi_2$ in Ar-atmosphere. At

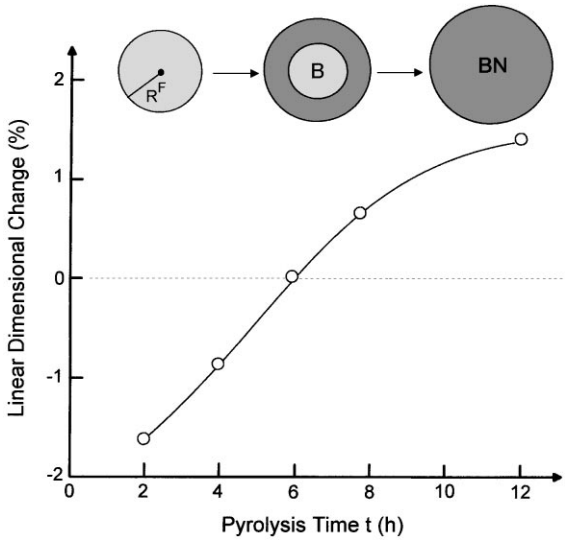

Fig. 4. Linear dimensional change of poly(sitoxane)/40 vol% B mixture pyrolyzed at 1480°C in nitrogen atmosphere as a function of filler reaction time.

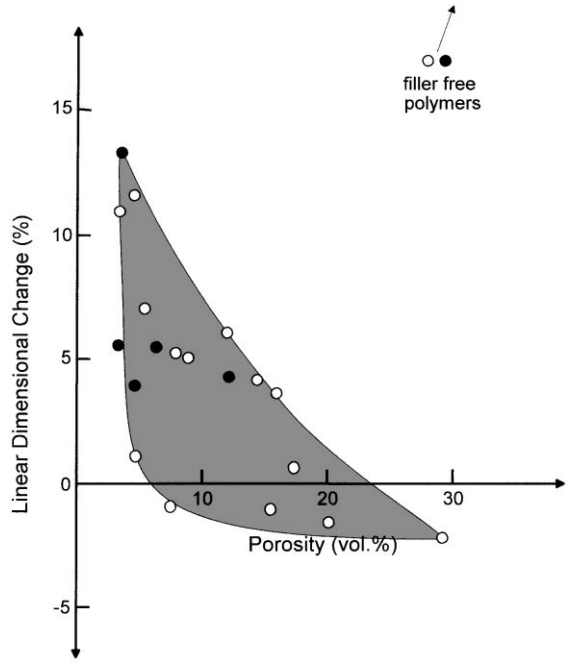

Fig. 5. Shrinkage versus porosity of various poly(siloxane)/ active filler systems pyrolyzed at 1200–1400°C in nitrogen atmosphere (○) poly(methylsiloxane); (●) poly(phenylsiloxane).

temperatures above 400°C an open pore channel network is formed in the low viscous polymer which, upon further heating to 1200°C, can diminish (transient porosity) by viscous sintering similar to gel-pore closure.[41] In inert Ar-atmosphere a second generation of open porosity is found in the Si–O–C-matrix derived from the carbon rich poly(vinylmethylphenylsiloxane) due to carbothermal reduction of SiO_2, above 1200°C by C[23]

$$SiO_2(s) + C(s) \rightarrow SiO(g) + CO(g) \qquad (9)$$

$$SiO_2(s) + 3C(s) \rightarrow SiC(s) + 2CO_g \qquad (10)$$

which forms upon precipitation from the Si–O–C glass, eqn (1). In a reactive N_2-atmosphere, however, further reduction of total porosity can be

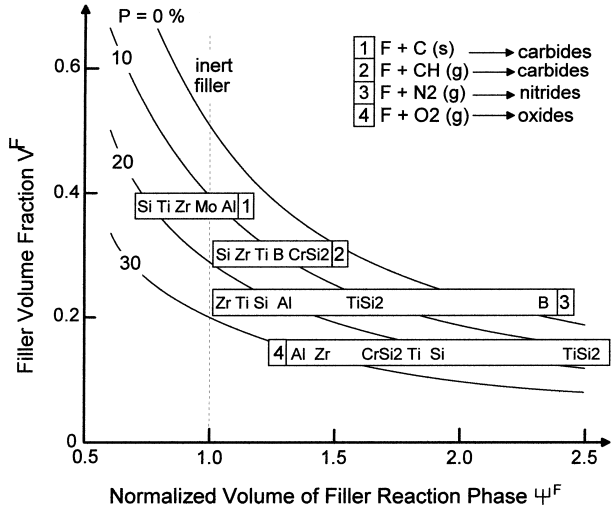

Fig. 6. Critical filler volume fractions to achieve zero shrinkage as a function of specific filler volume change calculated from eqn (8).

associated with matrix nitridation. Among the various filler materials $CrSi_2$ is of significant importance because it was found to enable nitridation of the polymer derived Si–O–C-phase and SiC via a Cr-catalyzed reaction according to[42]

$$\mathrm{Si-O}_a\mathrm{-C}_b\,(s) + N_2\,(g) \xrightarrow{Cr} Si_3N_4\,(s) + a\,CO\,(g) + (b-a)\,C\,(s)$$

$$3\,SiC\,(s) + 4\,N_2\,(g) \xrightarrow{Cr} Si_3N_4\,(s) + 3\,C\,(s)$$

which accounts for the transformation of most of the open porosity into closed porosity. Figure 8 shows the pore size distribution and the character of porosity of a $CrSi_2$-loaded poly(vinylmethylphenylsiloxane) pyrolyzed in nitrogen atmosphere of 1 MPa between 1100°C and 1500°C.

Porosity transformation and reduction of total porosity can be described according to the models for viscous sintering of glasses and gels derived by Mackenzie-Shuttleworth[43] and Scherer.[41] According to the cylindrical model derived by Scherer, isothermal sintering in the intermediate stage up to a relative density of 0·94 (interconnected pores open to atmosphere) can be described by

$$\int_0^t \frac{\gamma_{sv} n^{1/3}}{\eta}\,dt = \int_{x_0}^{x} \frac{2dx}{\left(3\pi - 8\sqrt{2x}\right)^{1/3} x^{2/3}} \qquad (11)$$

where x is given by the dimensions of a representative unit cell with $x = a/l$ (1 is the cell length and a is the cylinder radius). x defines the relative density ρ_{rel} (= bulk density over skeleton density $\rho_{rel} = \rho_b/\rho_s$) by

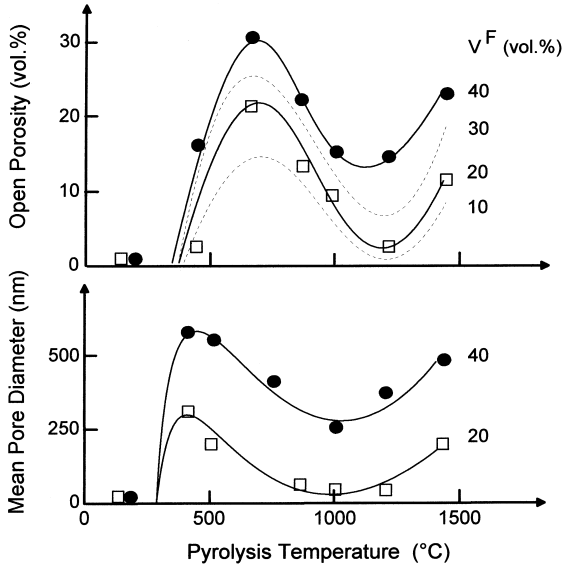

Fig. 7. Porosity and pore size development during reaction pyrolysis in argon atmosphere of poly(phenyisiloxane) filled with $CrSi_2$, (mean particle size 2 μm).[42]

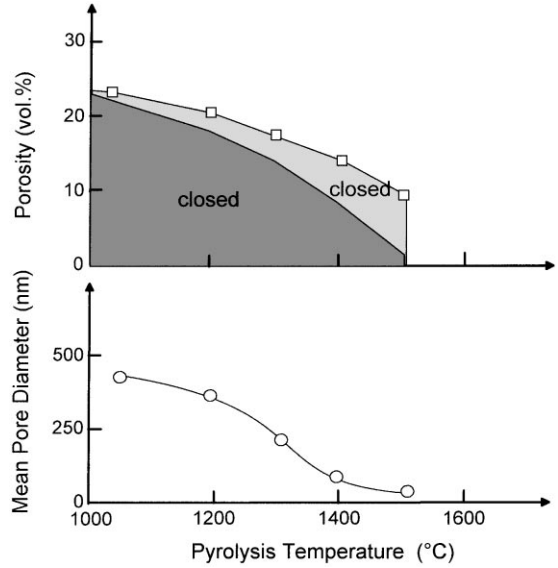

Fig. 8. Porosity and pore size development of poly(-phenylsiloxane) filled with 40 vol% of $CrSi_2$ during pyrolysis in reactive nitrogen atmosphere.[42]

$$\rho_{\text{rel}} = x^2(3\pi - 8\sqrt{2x}) \tag{12}$$

Using eqn (11) densification rate can be adequately described by

$$\frac{\mathrm{d}\rho}{\mathrm{d}t} \approx \frac{\gamma_{sv} n^{1/3}}{\eta} \tag{13}$$

where γ_{sv} represents the specific surface energy and η the viscosity. n equals the number of pores per unit volume and is given as a function of the relative density ρ_{rel}, and the pore radius, r_p,

$$\frac{n^{1/3} \approx m\left(\frac{1}{\rho_{\text{rel}}} - 1\right)}{r_p} \tag{14}$$

m is a constant (0·62 according to the Mackenzie-Shuttleworth model). Large volume fractions of the filler seem to be responsible for significantly larger pore sizes r_p, when the polymer starts to decompose, Fig. 7. Since smaller pores tend to shrink significantly faster compared to larger pores, eqns (13) and (14), shrinkage rate and hence final porosity was found to be smaller in the systems containing less filler. The viscous sintering models shows that pore shrinkage accelerates with decreasing viscosity η. In contrast to glasses where η decreases with increasing temperature according to the Vogel–Futcher–Tamman relation the polymer derived Si–O–C phase may exhibit an increase in viscosity due to crystallization of the amorphous Si–O–C phase into SiC and SiO_2, at temperatures above 1100°C, eqn (1). In addition, the rigid filler network results in an increasing stiffness of the composite with increasing filler content so that hydrostatic tensile stresses impede densification of the constrained matrix phase.[44,45] Thus, viscosity is not a single valued function of temperature but a complex function of irreversible phase formation reactions and thermal history during reaction pyrolysis.

3.3 Microstructure and properties

The mcrostructure of the pyrolyzed ceramic composites consists of a residual porosity, a filler derived carbide, nitride or oxide reaction phase and the polymer derived Si–O–C(−N) matrix phase. Figure 9 shows a typical microstructure of a poly(phenylsiloxane)/CrSi,-mixture pyrolyzed in nitrogen atmosphere at 1400°C.[42] The filler reaction product is Cr_3C_2/Si_3N_4 (bright) which is homogeneously embedded in the polymer derived Si-O-C-N phase (dark). From the polymer derived amorphous phase nanoparticles of crystalline silicon carbide, silicon oxide or silicon nitride, respectively, precipitate at temperatures above 1000–

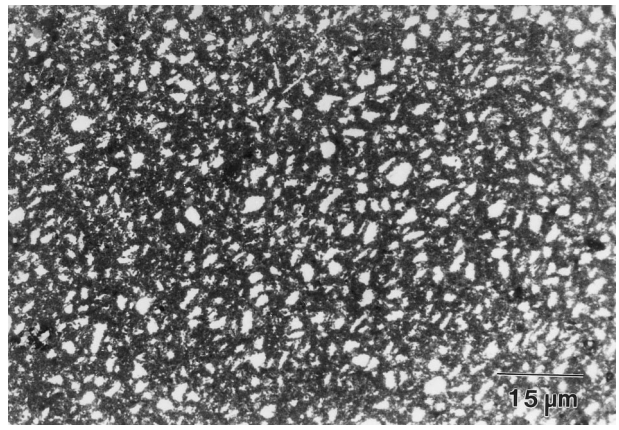

Fig. 9. Micrograph of polished surface of poly(phenylsiloxane)/$CrSi_2$ mixture pyrolyzed at 1400°C in nitrogen atmosphere (s. text).

1400°C. In the case carbon rich polymers are used, an additional network of turbostratic carbon may be formed above 800°C so that a complex microstructure with two distinct particle size populations in the matrix (< 100 nm) and the filler reaction phase (0·1−1 μm) is generated, Fig. 10. The material properties of the pyrolyzed ceramic microcomposites are dominated by the interaction of the various interpenetrating networks in the hierarchical microstructure. Generally the material properties may be distinguished into properties varying continously with volume fraction of filler phase and into properties, which exhibit a nonlinear change at a critical percolation threshold. Figures 11 and 12 show the bending strength of various polysiloxane/filler-derived ceramics as a function of filler volume fraction and of residual porosity, respectively. Modulus of rupture, MOR, increases almost linearly with increasing filler volume fraction V^F up to a maximum filler fraction

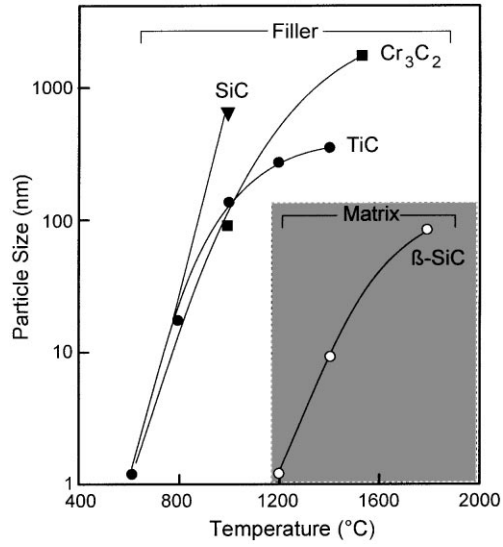

Fig. 10. Particle sizes in polymer/filler-derived ceramics with hierarchical microstructure.

$V_{max}{}^F$ beyond which a pronounced decrease is found. Above $V_{max}{}^F$ packing density of the filler particles is high enough to avoid rearrangement upon polymer pyrolysis so that the rigid filler network can no more compensate for the polymer induced shrinkage resulting in a pronounced increase of large size porosity.

Dependence of rupture strength on porosity P can be described based on minimum solid area type models.[46] Regression analysis of strength - porosity data in the $CrSi_2$ and $MoSi_2$ containing polymer systems yields an exponential relation

$$MOR = MOR_0 \exp(-5P) \qquad (15)$$

where MOR_0 is the extrapolated rupture strength of the fully dense material which equals 630 MPa . The major difference between inert and active fillers can be associated to the reduction of porosity which, according to eqn (15) explains the higher strength of polymer derived ceramics loaded with active fillers compared to inert filler containing systems.

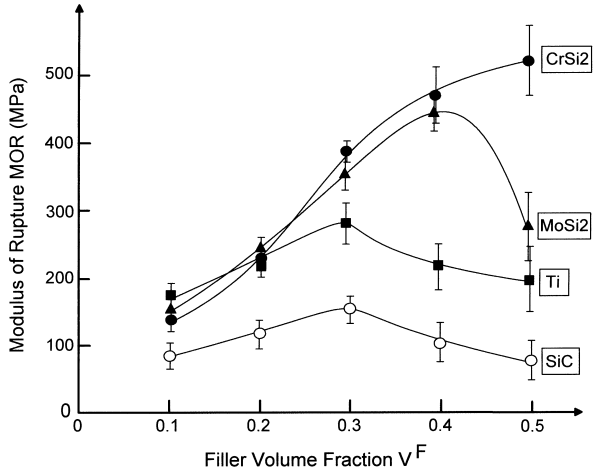

Fig. 11. Strength of poly(siloxane)/filler derived ceramics as a function of filler content.

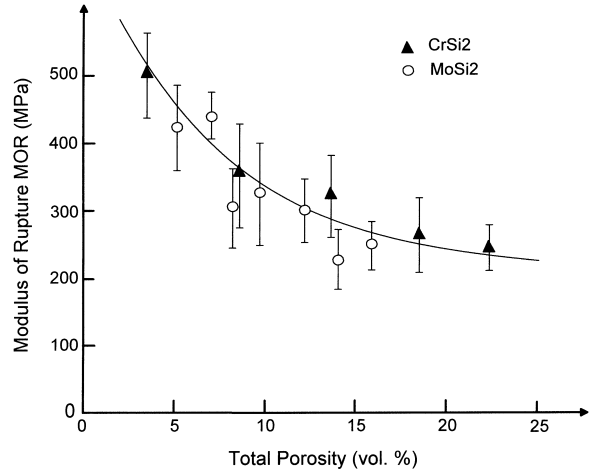

Fig. 12. Strength of poly(siloxane)/filler derived ceramics versus total porosity.

In contrast to strength and thermal expansion shown above, the electrical conductivity of the polymer/filler derived ceramics strongly depends on the formation of a percolation network. The filler reaction phase forms a threedimensionally interconnected network when the inital filler volume fraction exceeds a critical percolation limit. According to the model of Janzen [47] the critical filler loading for continous network formation, V_N^F, is

$$V_N^F \approx \left[1 + \frac{Z}{C_p}\left(\frac{1 - V_c^F}{V_c^F}\right)\right]^{-1} \qquad (16)$$

where C_p is the critical number of contacts per particle and Z the maximum number of contacts. For the case of randomly oriented spherical particles (in which C_p equals 1·5 and Z equals 6) and $V_c^F = 0{\cdot}5$ a critical network forming filler fraction of $V_N^F = 0{\cdot}2$ results from eqn (16). For inhomogeneous distribution of the filler particles the percolation threshold may be higher due to cluster formation. Figure 13 shows the volume fraction of conductive filler $Mosi_2$ ($\rho_{RT} = 2 \times 10^{0{\cdot}5}\Omega$ cm) plotted vs. the electrical resisitvity of a composite pyrolyzed at 800°C where no filler reaction has occurred. At filler volume fractions below 30 vol% the material is an insulator ($\rho_{RT} \geq 10^{13}\Omega$ cm). At higher filler volume fractions a sharp decrease results in an insulator-conductor transition with an electrical resistance similar to $MoSi_2$ Replacing $MoSi_2$ by non-conducting filters such as Si_3N_4 or Al_2O_3 it is possible to adjust the electrical properties in a wide range between insulating and conducting behavior.

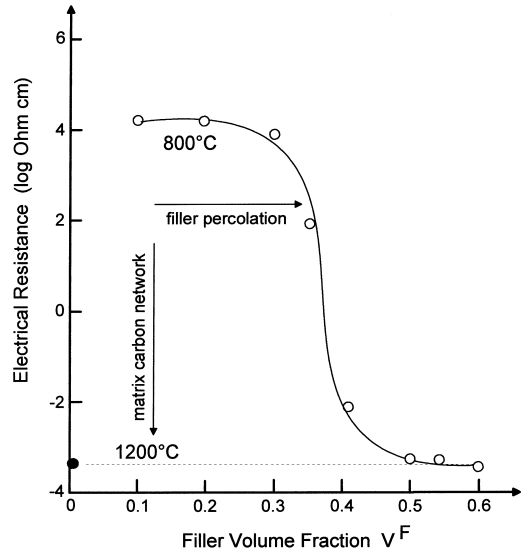

Fig. 13. Electrical (DC) resistance at room temperature for poly(phenylsiloxane)/$MoSi_2$(3 μm) system pyrolyzed at 800°C and for filler free poly(phenyisiloxane)pyrolyzed at 1200°C.

3.4 Conclusions

Bulk ceramic components can be manufactured with low or even zero dimensional change by active filler controlled polymer pyrolysis process. Mechanical, tribological and other physical and chemical properties may well be tailored by the type and distribution of the filler phase and the reaction conditions. Based on low price poly(-siloxane) polymers various applications in the fields of high temperature furnace technology, mechanical engineering and automobile technology are currently investigated. Ceramic composite materials derived from preceramic polymer-filler mixtures are of particular interest for wear resistant machinery components, fiber-reinforced, lightweight components for aircraft structures, surface sealing of porous components and even biomedical dental restorations. Extending the polymer/active filler approach to systems containing additional fillers with special physical properties and which remain stable during pyrolysis, a novel group of materials with specific electrial, thermal, magnetical or biological functionality can be synthesized.

Acknowledgements

Financial support for part of this work from German Ministry for Science and Technology (BMBF) and German Science Foundation (DFG) is gratefully acknowledged.

References

1. Chantrell, P. G. and Popper, P., Inorganic polymers for ceramics In *Special Ceramics*, ed. P. Popper. Academic Press, New York, 1960, pp. 67.
2. Yajima, S., Hayashi, J., Omori, M. and Okamura, K., Development of tensile strength silicon carbide fiber using organosilicon polymer precursor. *Nature*, 1976, **261**, 683.
3. Rice, R. W., Ceramics from polymer pyrolysis, opportunities and needs—a materials perspective. *Am. Ceram. Soc. Bull*, 1983, **62**, 889.
4. Wills, R. R., Markle, R. A. and Mukherjee, S. P., Siloxanes, silanes, and silazanes in the preparation of ceramics and glasses. *Am. Ceram. Soc. Bull*, 1983, **62**, 904.
5. Shilling, C. L., Wesson, J. P. and Williams, T. C., Polycarbosilane precursors for silicon carbide. *Am. Ceram. Soc. Bull*, 1988, **62**, 9–12.
6. Wynne, K. J. and Rice, R. W., Ceramics via polymer pyrolvsis. *Ann. Rev. Mat. Sci*, 1984, **14**, 297.
7. West, R. Polysilane precursors to silicon carbide. In *Ultrastructure Pocessing of Ceramics, Glasses and Composites*, ed. L. L. Hench and D. R. Ulrich. Wiley Interscience, New York, 1984, pp. 235.
8. Seyferth, D., Wisemann, G. H., Schwark, J. M., Yu, Y. F. and Poutasse, C. A., Organosilicon polymers as precursors for silicon-containing ceramics. In *Inorganic and Organometallic Polymers, Am. Ceram. Soc. Symp. Series*, 1987, **360**, 143.
9. Pouskouleli, G., Metalorganic compounds as preceramic materials, 1. Non-oxide ceramics. *Ceram. Int*., 1989, **15**, 213.
10. Peuckert, M., Vaahs, T. and Brueck, M., Ceramics from organometallic polymers. *Advanced Materials*, 1990, **2**, 398.
11. Rahn, J. A., Laine, R. M. and Zhang, Z. F., The catalytic synthesis of inorganic polymers for high-temperature applications and as ceramic precursors. *Mat. Res. Soc. Symp. Proc*, 1990, **171**, 31.
12. Lipowitz, J., Polymer-derived ceramic fibers. *Am. Ceram. Soc. Bull*, 1991, **70**, 1888.
13. Reniund, G. R., Prochazka, S. and Doremus, R. H., Silicon oxycarbide glasses: Part 1. Preparation and chemistry: Part 11. Structure and properties. *J. Mat. Res*, 1991, **6**, 2716 and 2723.
14. Baldus, H. P., Wagner, O. and Jansen, M., Synthesis of advanced ceramics in the system Si–B–N and Si–B–N–C employing novel precursor compounds. In *Mat. Res. Soc. Symp. Proc*, 1992, **271**, 821.
15. Riedel, R., Passing, G., Schönfelder, H. and Brook, R. J., Synthesis of dense silicon-based ceramics at low temperatures. *Nature*, 1992, **355**, 355.
16. Atwell, W. H., Burns, G. T. and Zank, G. A., Silicon carbide preceramic polymers as binders for ceramic powders. In *Inorganic and Organometallic Oligomers and Polymers*, ed. J. F. Harrod, R. M. Laine, Kluwer, Dordrecht Netherlands, 1991, pp. 147.
17. Yajima, S., Okamura, K., Shishido, T., Hasegawa, Y. and Matsuzawa, T., Joining of SiC to SiC using polyborosiloxane. *Am. Ceram. Soc. Bull*, 1983, **60**, 253.
18. Burns, G. T. and Chandra, G., Pyrolysis of preceramic polymers in ammonia: preparation of silicon nitride powders. *J. Am. Ceram. Soc*, 1989, **72**, 333.
19. Walker, B. E., Rice, R. W., Becher, P. F., Bender, B. A. and Coblenz, W. S., Preparation and properties of monolithic and composite ceramics produced by polymer pyrolysis. *Am. Ceram. Soc. Bull*, 1983, **62**, 916.
20. Jamet, J., Spann, J. R., Rice, R. W., Lewis, D. and Coblenz, W. S, Ceramic fiber composite processing via polymer-filler matrices. *Ceram. Eng. Sci. Proc*, 1984, **5**, 677.
21. Hurwitz, F. I., Gyenkenyesi, J. Z. and Conroy, P. J., Polymer-derived nicalon/Si–C–O composites: processing and mechanical behavior. *Ceram. Eng. Sci. Proc*, 1989, **10**, 750.
22. Yajima, S., Hayashi, J. and Imori, M., Continous silicon carbide fiber of high-temperature strength. *Chem. Lett*, 1957, **9**, 931.
23. Cook, T. F., Inorganic fibers—A literature review. *J. Am. Ceram. Soc*, 1991, **74**, 2959.
24. Greil, P., Active-filler-controlled pyrolysis of preceramic polymers. *J. Am. Ceram. Soc*, 1995, **78**, 835.
25. Greil, P. and Seibold, M., Modelling of dimensional changes during polymer-ceramic conversion for bulk component fabrication. *J. Mat. Sci*, 1992, **27**, 1053.
26. Erny, T., Seibold, M., Jarchow, O. and Greil, P., Microstructure development of oxycarbide composites during active filler controlled polymer pyrolysis. *J. Am. Ceram. Soc*, 1993, **76**, 207.
27. Seibold, M. and Greil, P., Thermodynamics and microstructural development of ceramic composite formation by active filler controlled pyrolysis (AFCOP). *J. Europ. Ceram. Soc*, 1993, **11**, 105.
28. Walter, S., Suttor, D., Erny, T., Hahn, B. and Greil, P., Injection moulding of polysiloxane/filler mixtures of oxycarbide cramic composites. *J. Europ. Ceram. Soc*, 1996, **16**, 387.
29. Suttor, D., Erny, T., Greil, P., Goedecke, H. and Haug, T., Fiber-reinforced ceramic-matrix composites with a polysiloxane/boron-derived matrix. *J. Am. Ceram. Soc*, 1997, **80**, 1831.
30. Colombo, P., Abdirashid, M. O., Maddalena, A. and Marchetti, A., Aluminium powder preceramic polymer mixtures for the preparation of ceramic composites. In *Fourth Euro Ceramics*, Vol. 4, ed. A. Bellosi, Gruppo Editorale Faenza Editrice SpA., Italia, 1995, pp. 117.

31. Yu, S. H., Riman, R. E., Danforth, S. C. and Leung, R. Y., Pyrolysis of titanium-metal-filled poly(siloxane) preceramic polymers: effect of atmosphere on pyrolysis product chemistry. *J. Am. Ceram. Soc*, 1995, **78**, 1818.
32. Lightfoot, A., Haggerty, J. S. and Rhine, W. E., Ceramic matrices and monoliths synthesized from a combination of reactive polymers, filters and atmospheres. In *Proceedings of the 19th Annual.Conference on Composites and Advanced Ceramics*. Am. Ceram. Soc., Cocoa Beach, FL, January, 1995, paper 95-02.
33. Jiang, Z. and Rhine, W. E., Preparation of nanophase SiC/Si_3N_4, SiC/B_4C and stochiometric SiC from mixtures of a vinylic polysilane and metal powders.*Mat. Res. Soc. Symp. Proc*. Vol. 286, Mat. Res. Soc., 1993, pp. 437.
34. Seyferth, D., Bryson, N., Workman, D. P. and Sobon, C. A., Preceramic Polymers as Reagents in the preparation of ceramics. *J. Am. Ceram. Soc*, 1991, **74**, 2687.
35. Jakubenas, K. and Marcus, H. L., Silicon carbide from laser pyrolysis of polycarbosilane. *J. Am. Ceram. Soc*, 1995, **78**, 2263.
36. Bond, G. C., *Catalysis of metals*. Academic Press, London, 1964.
37. Jenkins, G. and Kawamura, K., Polymeric carbons—Carbon Fiber, Glass and Char, Cambridge University Press, Cambridge, UK, 1976.
38. Bouillon, E., Langlais, F., Pailler, R., Naslain, R., Cruege, F., Huong, P. V., Sorthou, J. C., Delpuech, A., Laffon, C., Lagarde, P., Monthioux, M. and Oberlin, A., Conversion mechanisms of polycarbosilane precursor into an SiC-based ceramic material. *J. Mat. Sci*., 1991, **26**, 1333.
39. Levenspiel, O., *Chemical reaction engineering*. Wiley, New York, 1972.
40. Lipowitz, J., Rabe, J. A., Frevel, L. K. and Miller, R. L., Characterization of nanoporosity in polymer-derived ceramic fibers by X-ray scattering techniques. *J. Mat. Sci*., 1990, **25**, 2118.
41. Scherer, G. W., Sintering of low-density glasses. *J. Am. Ceram. Soc*, 1997, **60**, 236.
42. Erny, T., Formation, structure and properties of polymer derived composite ceramics in the system $MeSi_2$,/polysiloxane, PhD Thesis, University of Erlangen, Germany, 1996 (in German).
43. Mackenzie, J. K. and Shuttleworth, R., Phenomenological theory of sintering. *Proc. Phys. Soc. London*, 1949, **62**, 833.
44. Bordia, R. K. and Scherrer, G. W., On constrained sintering—I. Constitutive model for a sintering body. *Acta Metall*., 1988, **36**, 2393.
45. De Jonghe, L. C. and Pahaman, M. N., Sintering stress of homogeneous and heterogeneous powder compacts. *Acta Metall*., 1988, **36**, 223.
46. Rice, R. W., Evaluation and extension of physical property—porosity models based on minimum solid area. *J. Mat. Sci*., 1996, **31**, 102.
47. Jantzen, J., On the critical conductive filler loading in antistatic composites. *J. Appl. Phys*., 1975, **46**, 966.